American Mineralogist, Volume 83, pages 451–457, 1998

Possible polytypism in FeO at high pressures

Igor I. Mazin,* Yingwei Fei, Robert Downs,† and Ronald Cohen

Geophysical Laboratory and Center for High Pressure Research, Carnegie Institution of Washington, 5251 Broad Branch Road, N.W., Washington, D.C. 20015, U.S.A.

Abstract

Examination of X-ray diffraction intensities for FeO collected in situ at high pressure and high temperature reveals that the atomic arrangements of FeO in the hexagonal structure are not the same as those in the simple NiAs-type structure (B8) where Fe takes the place of Ni. The observed diffraction intensity can be explained by adding an anti-B8 component (where Fe takes the place of As). Substitution of Fe and O atoms for each other is crystallochemically unique. The exchange of Fe and O positions provides a critical measure of the change in chemical bonding. Our conclusion is consistent with the observed transition of FeO from an ionically bonded structure to a strongly covalent and metallic one. First-principles electronic structure computations using the linearized augmented plane wave (LAPW) method with the generalized gradient approximation (GGA) indicate that both B8 and anti-B8 should be antiferromagnetic, but only anti-B8 should be an insulator. The GGA and local density approximation (LDA) incorrectly compute anti-B8 as the ground state structure.

Introduction

FeO is a major component of the Earth, due to solid solution with magnesiowüstite, believed abundant in the lower mantle and believed to be enriched in the lowermost mantle (D″ region) (Jeanloz and Lay 1993). Important properties of the deep Earth, such as the electrical conductivity, may be controlled by the FeO component. Understanding of FeO is also important for crystal chemistry (Fei 1996). At low pressures there is nearly ideal solubility of Fe^{2+} for Mg^{2+} in most minerals, which is surprising because Mg^{2+} is a simple closed-shell ion, whereas Fe^{2+} is open shelled and FeO is a Mott insulator, one of a set of exotic transition metal compounds that is insulating due to strong local correlations in electron motions. At high pressures the ionic nature of Fe^{2+} changes and becomes more covalent (Cohen et al. 1997) and will probably not exchange so easily with Mg^{2+}, which would have important implications for geochemistry, but exactly how this change happens is unclear. Jeanloz and Ahrens (1980) and Knittle and Jeanloz (1986) found a high-pressure, high-temperature phase transition in FeO to a metallic phase, evidence for the change in Fe^{2+} character at high pressures. Fei and Mao (1994) determined the structure to be based on NiAs from in situ high-pressure, high-temperature X-ray diffraction. However, the observed diffraction intensities were not consistent with the expected values for a single NiAs-type structure.

Understanding FeO is also important for the development of solid-state theory (Mazin and Anisimov 1997 and references therein). Most forms of band theory predict FeO to be a metal, whereas it is observed to be an insulator. Several methods that include effective local Coulomb interactions neglected in GGA and LDA such as Hartree-Fock (Mackrodt et al. 1993), SIC (Szotek and Temmerman 1993), or LDA+U (Anisimov et al. 1991; Mazin and Anisimov 1997), or local models (Takahashi and Igarashi 1996) give a band gap, but whether they reproduce the proper high-pressure behavior (a metal-insulator transition) is unknown.

A reexamination of the X-ray diffraction data of FeO and new theoretical computations suggested that the high pressure phase diagram may be more complicated than previously thought. New crystallochemical behavior is suggested, where anions and cations substitute for each other, which has not been seen previously in an oxide.

X-ray diffraction intensities

At ambient pressure FeO assumes the cubic rocksalt (B1) structure, which can be viewed as two interpenetrating face-centered cubic (fcc) sublattices of Fe and O. Another useful visualization of this structure is one of close-packed planes stacked in the [111] direction, with the stacking sequence being, in traditional crystallographic notation, AbCaBcAbCaBc, where lower case letters stand for planes of Fe atoms and upper case letters for planes of O atoms. At low temperature, FeO displays a rhombohedral distortion (rhombohedral angle $\alpha < 60°$),

* Present address: Naval Research Laboratory, Washington, D.C. 20375, U.S.A., and CSI, George Mason University, Fairfax, Virginia 22030, U.S.A.

† Present address: Department of Geosciences, Gould-Simpson Building, University of Arizona, Tucson, Arizona 85721, U.S.A.

0003–004X/98/0506–0451$05.00

which increases with pressure (Yagi et al. 1985). The distortion results in a shortened Fe-Fe distance. Electronic structure computations show that the distortion is due to an increase in metal-metal bonding with pressure (Isaak et al. 1993). The physical reason for this effect is that direct electronic hopping between Fe contributes substantially to the binding energy of the crystal. This contribution has covalent character and results in the decrease in the interplanar Fe-Fe distances. The magnitude of the Fe-Fe interactions increases with pressure, causing an increase in the rhombohedral distortion and eventually leading to the B1 $\rightarrow$ B8 transition with pressure. In the distorted structure the distance d between (111) planes increases with respect to the nearest neighbor distance a, whereas in the cubic structure the ratio of d to a is fixed, $d/a = \sqrt{2/3} \approx 0.816$. The maximum experimentally observed distortion (Yagi et al. 1985), $\alpha \approx 53.8°$, corresponding to $d/a \approx 0.94$, was found at the highest compression attained in that experiment and was estimated to be about 25% in volume. At about the same compression a phase transition to a hexagonal structure was observed (Fei and Mao 1994) at high temperatures (600 K at 96 GPa), which was interpreted to be a NiAs-type (B8) structure (Fig. 1). The experimentally determined c/a ratio was 2.0, or $d/a = 1.0$, slightly larger than in the rhombohedral phase at maximal compression. The transition discovered by Fei and Mao (1994) represents a change of symmetry due to a different stacking sequence of the close-packed monolayers, with the nearest-neighbor distances being essentially the same in both structures. This result suggests that stacking faults easily form in both structures.

The observed d spacings for the energy dispersive powder pattern of FeO at 96 GPa and 800 K (Fei and Mao 1994) match expected values for a B8 structure quite well, providing cell parameters of $a = 2.574(2)$ and $c = 5.172(4)$ Å. However, intensities computed under the assumption of a B8 structure do not match the observed ones very well at all. The discrepancy in intensity cannot be simply explained by preferential orientation of the sample, because an orientation that would increase the (101) intensity with respect to those of (100) and (102), would lead to near total extinction of the (002) and (004) peaks.

The B8 structure can be considered as a distorted hexagonal closest-packed analogue of rock salt (B1) with one atom located at [000] and the other at [⅔, ⅓, ¼] under $P6_3/mmc$ symmetry. In the NiAs structure, Ni is assigned to the position at the origin, resulting in nearest neighbor Ni-Ni separations (2.53 Å) that are quite a bit smaller than those for As-As (3.28 Å). However, for FeO in the B8 structure, with a much larger c/a ratio, the nearest neighbor Fe-Fe distances and O-O distances are the same, 2.57 Å. This removes the necessity of placing Fe at the origin, and so we must consider both possibilities, the B8 structure, with Fe at the origin, and the anti-B8 structure, with O placed at the origin.

Consequently, theoretical energy dispersive powder diffraction patterns for B8 and anti-B8 were computed to determine the structural state of FeO at 96 GPa and 800 K. Diffraction patterns of FeO, Au, and a background were computed and fit to the observed pattern using a modified version of XPOWPLOT (Downs et al. 1993) and the strategies outlined by Reynolds (1985). Au had been included in the cell to enable the determination of pressure from its equation of state. The background was modeled as a series of diffuse peaks scattered from the diamonds with cell parameters ranging from those at room condition to those at 96 GPa. The computed intensities for the patterns of all phases (B8, anti-B8, and Au) were summed and fitted to the observed intensities by varying a scale factor and peak-width parameter for each pattern under the assumption of Gaussian peak shapes.

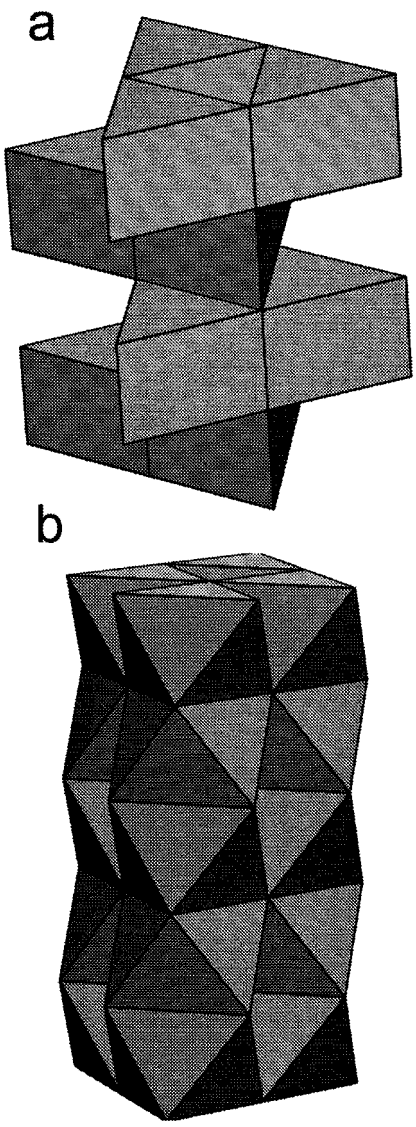

FIGURE 1. Crystal structure of NiAs (B8) structure, (**a**) polyhedral representation around As atoms, and (**b**) polyhedral representation around Ni atoms.

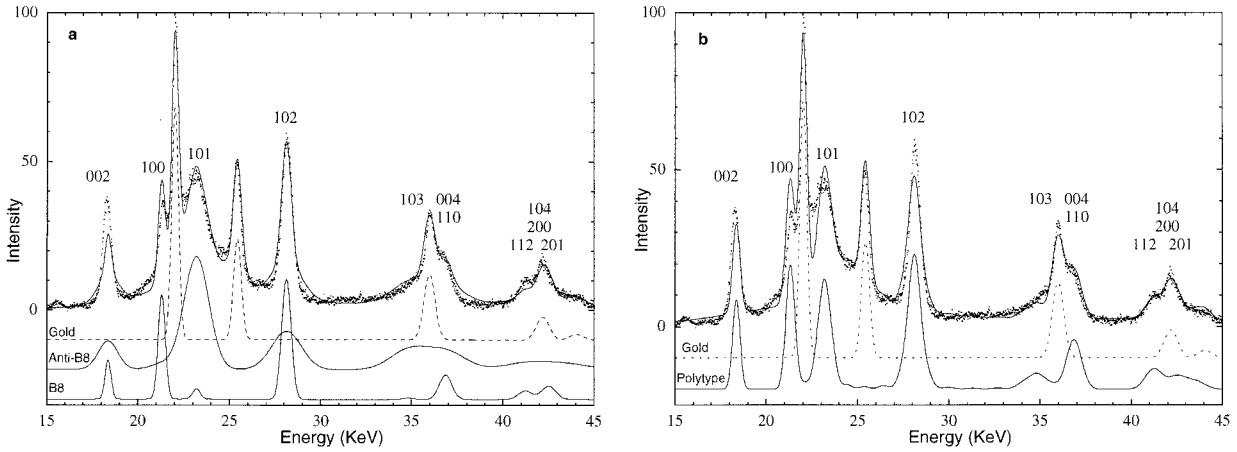

FIGURE 2. Comparison of calculated and experimental spectra of B8-derived phases of FeO with unit-cell parameters a = 2.574 Å and c = 5.172 Å corresponding to 96 GPa and 800 K: (**a**) mechanical mixture of B8 (Fe→Ni, O→As) and anti-B8 (Fe→As, O→Ni) with equal amounts of each phase; and (**b**) polytype with 50% layers in B8 and 50% in the anti-B8 structure. Experimental data (dots) were collected in situ with energy-dispersive technique (2θ = 15°) (Fei and Mao 1994). Calculated energy dispersive diffraction patterns for Au (dashed line), anti-B8, B8, and polytype stacking of B8 and anti-B8 are shown below the observed spectrum with background removed. The *hkl* indices for hexagonal FeO are indicated.

The best fit for a mechanical mixture of B8 and anti-B8 was obtained with equal amounts of each phase, but with the peak widths of anti-B8 3.2 times larger than the peak widths of B8 (Fig. 2a). The results were somewhat satisfactory except for the inability to correctly match the observed peak widths at the shoulders of the FeO peaks: for instance, at 18.4, 28.1, 36.9, and 41.2 eV, and the fact that the fitted peak widths differ widely between the two phases. If the sample does consist of a mixture of B8 and anti-B8 crystals, the values of the fitting parameters suggest that whereas B8 and anti-B8 form in equal amounts, the anti-B8 phase is not as well crystallized as the B8 phase or much finer grained.

Another possibility is whether the mismatch of the shoulders on the FeO peaks could result from a polytype stacking of B8 and anti-B8. Therefore, a series of model polytype stacking sequences were computed and fit to the observed pattern. The fitting procedure was the same as for the mechanical mixture, except the number of parameters is smaller because the polytype was fit with only one scale factor and one peak width. The best fit was obtained by stacking five layers of B8 and then five layers of anti-B8; in a 5:5 sequence (Fig. 2b). It is reasonable that the stacking would be made of equal amounts of both phases because the mechanical mixture model was fit best with equal amounts of each phase. For stacking sequences smaller than 5:5, for instance, 3:3 or 4:4, the computed peak widths are too large because the satellite peaks are too far from the main peaks. For stacking sequences larger than 5:5, for instance, 6:6 or 8:8, the peaks are too narrow because the satellites are drawn in too close to the main peak. Figure 2b shows an improved fit around the shoulders of the peaks, especially for the one at 41.2 eV. This peak could not be fit or reproduced in any other way except by some sort of polytype stacking. Thus we favor B8/anti-B8 polytypism rather than a mechanical mixture in FeO under high pressure, although confirmation requires more accurate intensity measurements. In any case, the observed diffraction pattern of FeO at high pressure and high temperature cannot be explained by a simple B8 structure.

Our suggested polytypism of FeO differs from typical polytypes such as ZnS and SiC (Rai et al. 1986). The average lattice in the B8 structure is double-layer hexagonal close-packed (dhcp) and the sublattices are crystallographically nonequivalent, so that interchanging components transform the lattice (B8) into another lattice (anti-B8) with different properties. This makes potential polytypism in such a material much richer than in those known before, allowing, for example, an infinite variety of polytypes with hexagonal stacking only (one can also say that there are two nonequivalent polytypes of the 2H kind) (see Rai et al. 1986). Note that in the latter case polytypism manifests itself only in the X-ray intensities, whereas peak positions are essentially the same for all polytypes. The stacking boundary in such a case is given by the following sequence: aCb**CaB**aCa. Neither sublattice makes a close-packed lattice. The average lattice is nevertheless close packed (dhcp with stacking faults).

It is instructive to consider an image of the B8/anti-B8 stacking boundary with nine layers at either side (Fig. 3). The central region (a stacking fault) is one layer of the B1 structure, which is distorted similar to the rhombohedral strain found in the rhombohedral phase depending on the layer spacings. We considered only uniform spacings so that the strained region would have d/a = 1, not too different from the observed maximal rhombohedral strain near the transition. Since the stacking fault region could be larger and still join together B8 and anti-B8 regions, one could have a continuous stacking transition

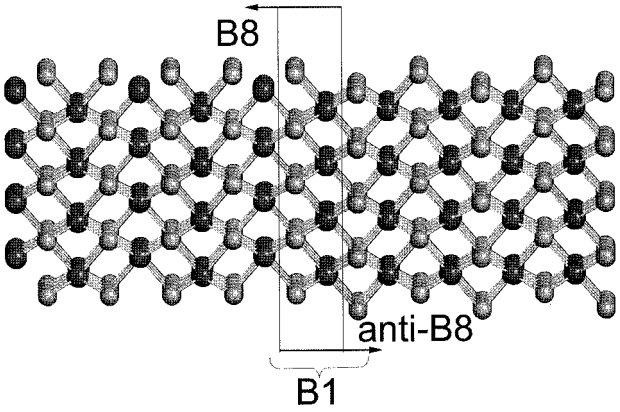

FIGURE 3. Image of the stacking boundary between the B8 and anti-B8 regions. The stacking boundary itself forms a distorted B1 (NaCl-type) structure.

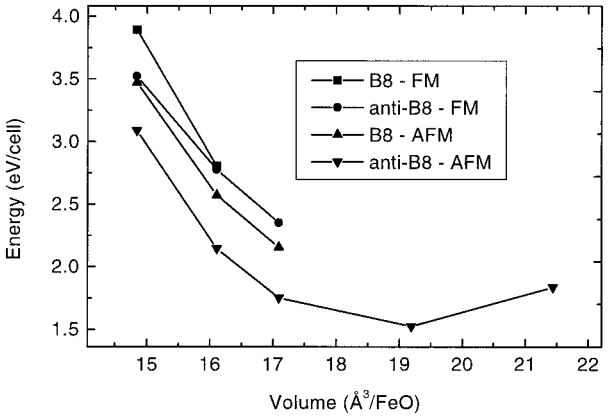

FIGURE 4. Total energies per cell (4 atoms) for B8 and anti-B8 with ferromagnetic (FM) and anti-ferromagnetic (AFM) ordering computed using the LAPW method within GGA.

among B1, B8, and anti-B8, or even mixed phases or complicated long-range superstructures. Because the physical properties would be strongly dependent on the stacking sequences, as discussed below, the properties of high-pressure FeO may be highly varied. Properties may depend on sample history, because stacking sequences might be metastable. The stability of such stacking faults depends on the stacking fault energies. Given the similarity of the *d*/*a* ratios of the B8 and anti-B8 found theoretically (see below) and the *d*/*a* of the rhombohedrally strained B1 near the transition, we suspect that stacking fault energies are not forbiddenly high. This inference is consistent with our conclusion that polytypism is the most probable interpretation of the present X-ray data.

TOTAL ENERGY BAND STRUCTURE COMPUTATIONS AND ELECTRONIC STRUCTURE

To better understand the energies and electronic structure of B8 and anti-B8, total energy calculations were performed using the linearized augmented plane wave method (Singh 1994; Wei and Krakauer 1985) similar to those described in Isaak et al. (1993), except using the Generalized Gradient Approximation (GGA) for the exchange-correlation energy (Perdew and Wang 1992). Results are shown in Figure 4.

We found that at a volume of 14.8 Å^3 (volumes and energies are per formula unit) corresponding to a pressure of ~96 GPa, ferromagnetic (FM) anti-B8 is more stable by 0.25 eV, but both structures have the same energy at the larger volume of 16.3 Å^3 (Fig. 4). However, the strong similarity between the cubic B1 and the B8 structure suggests that the ground state should be rather antiferromagnetic (AFM), although this possibility has never been discussed in the literature. Indeed, we found the AFM structure to be more stable than the FM for all volumes studied (14.8–17.2 Å^3) by 0.2–0.3 eV. This is similar to the AFM stabilization energy for B1 FeO (Isaak et al. 1993; Sherman and Jansen 1995). We find that AFM anti-B8 is substantially more stable than B8. Moreover, the energy difference remains at approximately 0.25 eV up to the largest volume studied, 17.2 Å^3. The calculated *c*/*a* ratios for B8 and anti-B8 are 2.016 and 2.022, respectively. Such a small difference in *c*/*a* ratio is not resolvable from our experimental data, which yielded a *c*/*a* ratio of 2.01. The small difference is consistent with a coherent interference of B8 and anti-B8.

The energy difference predicted between B8 and anti-B8 suggests that the stable phase is anti-B8, and B8 or the B8/anti-B8 polytype are metastable, and formed due to kinetics or applied stresses. However, the calculated AFM stabilization energy is larger than the energy difference between ferromagnetic B8 and AFM B1, given by Sherman and Jansen (1995), and we estimate a stabilization of 0.075 eV/Fe of anti-B8 over B1. The prediction of anti-B8 as the ground state rather than B1 is problematic, and seems to contradict experimental results. The theoretical calculations are for pure FeO, but the entropic stabilization of $Fe_{0.92}O$ gives a free energy contribution of 0.072 eV at 1500K. Thus, it is possible that B1 FeO is stabilized at ambient pressure by non-stoichiometry. Recently Z. Fang et al. (unpublished manuscript) completed planewave pseudopotential computations on B8 and anti-B8 FeO and obtained similar results for FeO that density functional theory using present functionals predicts anti-B8 to be the zero pressure ground state for FeO rather than B1, suggesting that this result is robust and independent of LAPW implementation or calculation details. On the other hand, Fang et al. (1997) found LDA+U gives B1 as the ground state. These results point to the urgency of solving the transition-metal oxide problem, which is one of the major problems confronting computational solid state physics.

To further understand the behavior of FeO, band structures were computed using the LMTO-ASA method (Andersen 1975) within the GGA (Fig. 5). The characters of the bands show clearly that in the anti-B8, the spins are almost perfectly segregated on the two iron atoms in the cell, with one spin state occupied and the other not oc-

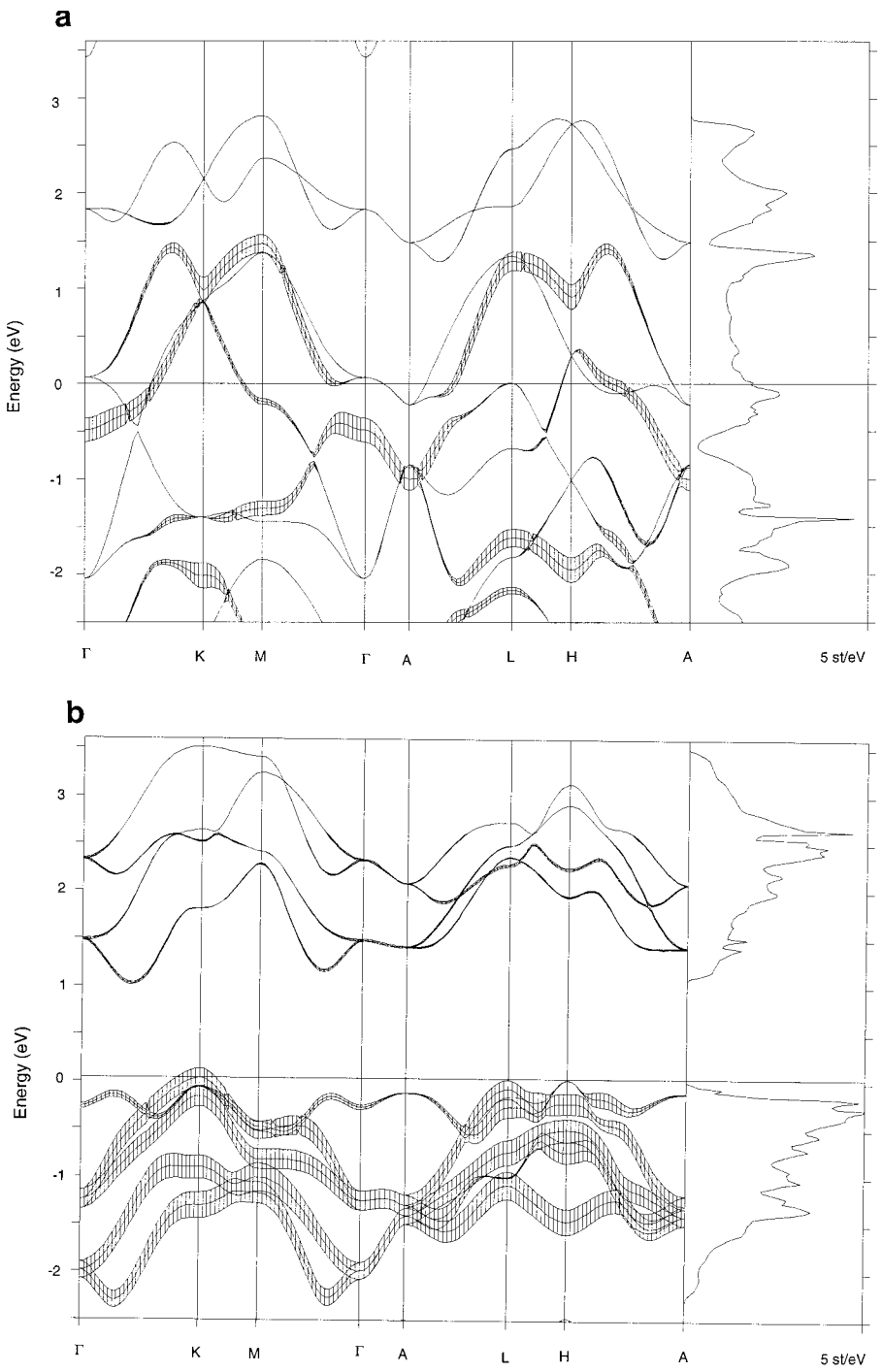

FIGURE 5. Band structures and densities of states at $V = 14.8$ Å^3 ($P = \sim 96$ GPa) computed using the LMTO-ASA method. The hatching width of the band represents the amount of spin-up character on one Fe. (**a**) B8 structure. This is a good metal due to the Fe-Fe interactions across the shared faces that leads to broad $3z^2$-r^2 states, and broadening of the spin occupations. (**b**) Anti-B8 structure. This is a good insulator with a very wide gap. The spin-up states are much narrower and are almost fully occupied on one Fe atom per cell. The density of states is per spin.

cupied. In B8, the spins are more even distributed and no gap is formed. In anti-B8, the Fe ions are much farther apart than in B8, and this is also a reason for the insulating behavior in anti-B8 compared with B8.

We can speculate why GGA overbinds the AFM anti-B8 relative to the other phases. On the one hand, anti-B8 is the only structure that appears insulating at moderate pressure in the density functional calculations; we find a gap of 1 eV at the experimental transition pressure of 96 GPa, with $V = 14.8$ Å^3 (Fig. 5). Probably, this structure is not overbound, but all other computed structures have a systematic error increasing their total energy because they give band structures with no gap. On the other hand, AFM stabilization energies calculated here resemble those found earlier for B1, with both phases being metallic in theory. The problem stems from the fact that for all of these structures at these pressures local electronic correlations (i.e., Mott behavior) are expected to be important (Cohen et al. 1997). In ordinary materials, such as Si, standard band theoretic methods give reasonable energy differences for metallic and insulating phases, but that may not be the case for Mott or charge-transfer insulators.

If anti-B8 is insulating, as theory predicts, we also must explain the experimental data that shows B8 FeO to be metallic (Knittle and Jeanloz 1986). Because the experimental samples are mixtures of B8 and anti-B8, only the B8 portions would be conducting. This would lead to very anisotropic conductivity in the mixed crystals; they would act like crystals with alternating insulating and conducting layers. However, only anti-B8 is insulating in theory with AFM ordering; FM anti-B8 is metallic. The origin of the gap in AFM anti-B8 is due to Fe-Fe interactions, and the filled bands are nearly entirely spin-up on one iron and spin-down on the other. Interactions in each spin subsystem increases the gap thus gaining one-electron energy. Without the gap, the one-electron energy gain would be less (cf. Mazin and Singh 1997). Because the gap requires AFM ordering, there would be an interesting metal-insulator transition at the Néel point and anti-B8 at high temperatures would be metallic.

Both the present and previous computations show that B8 and anti-B8 are high-spin, and the metallic nature of B8 has nothing to do with high-spin–low-spin transitions, which are predicted at higher pressures (Cohen et al. 1997). Predictions are for a transition at 200 GPa in pure FeO, but it may occur at lower pressures in magnesiowüstite. Recent experiments suggest magnetic collapse at about 100 GPa in FeO (Pasternak et al. 1997).

Implications for the Earth

Unique site occupancies in FeO may have important implications for the phase diagram, mechanical, and thermodynamics properties of FeO and magnesiowüstite at high pressure. The equilibrium phase diagram of FeO may be richer than anticipated, including more than one hexagonal modification, as well as a variety of polytype structures. In real conditions, both in the experiment and in the Earth's interior, one should expect formations of metastable regular and irregular polytypes, thus making the actual (metastable) phase diagram history-dependent. Abundant stacking faults and stacking boundaries may influence mechanical properties, such as shear moduli.

FeO is also complicated by non-stoichiometry, which can be represented as $Fe_{1-x}O$, and the non-stoichiometry affects many of its physical properties (Hazen and Jeanloz 1984). The conbination of non-stoichiometry, stacking faults, polytypism, and magnetic transitions makes FeO one of the most complex minerals known, whose unusual properties may cause anomalous behavior in Fe-rich regions of the deep Earth.

It has been proposed that the lowermost mantle (D″) is enriched in FeO (Jeanloz and Lay 1993) and that enhanced electrical and thermal conductivity may be important boundary conditions for the dynamics of the mantle (Manga and Jeanloz 1996). Our interpretation of the diffraction pattern of the high-pressure phase of FeO suggests the possibility of very anisotropic mechanical and electronic properties. Coupled with the possibilities of high-spin low-spin transitions in magnesiowüstite in D″ leads to the possibility of very complex and interesting behavior that may influence mantle dynamics in this sensitive boundary region.

Acknowledgments

This research was supported by NSF grants EAR-9418934 (R.E.C.) and EAR-9418945 (Y.F.) and the National Science Foundation Center for High Pressure Research. Computations were performed on the Cray J90/12-1024 at the Geophysical Laboratory supported by NSF grant EAR-9512627. We thank V.I. Anisimov, R.M. Hazen, A.I. Liechtenstein, H.-K. Mao, and C.T. Prewitt for helpful discussions.

References cited

Andersen, O.K. (1975) Linear methods in band theory. Physical Review, B12, 3060–3083.

Anisimov, V.I., Zaanen, J., and Andersen, O.K. (1991) Band theory and Mott insulators: Hubbard U instead of Stoner U. Physical Review, B44, 943–954.

Cohen, R.E., Mazin, I.I., and Isaak, D.G. (1997) Magnetic collapse in transition metal oxides at high pressure: Implications for the Earth. Science, 275, 654–657.

Downs, R.T., Bartelmehs, K.L., Gibbs, G.V., and Boisen, M.B., Jr. (1993) Interactive software for calculating and displaying X-ray or neutron powder diffractometer patterns of crystalline materials. American Mineralogist, 78, 1104–1107.

Fei, Y. (1996) Crystal chemistry of FeO at high pressure and temperature. In M.D. Dyar, C. McCammon, and M.W. Shaefer, Eds., Mineral Spectroscopy: A Tribute to Roger G. Burns, p. 243–254. The Geochemical Society, Special Publication No. 5.

Fei, Y. and Mao, H.-K. (1994) In situ determination of the NiAs phase of FeO at high pressure and temperature. Science, 266, 1668–1680.

Hazen, R.M. and Jeanloz, R. (1984) Wüestite ($Fe_{1-x}O$); a review of its defect structure and physical properties. Reviews of Geophysics and Space Physics, 22, 37–46.

Isaak, D.G., Cohen, R.E., Mehl, M.J., and Singh, D.J. (1993) Phase stability of wüstite at high pressure from first-principles LAPW calculations. Physical Review, B47, 7720–7720.

Jeanloz, R. and Ahrens, T.J. (1980) Equations of state of FeO and CaO. Geophysical Journal of the Royal Astronomical Society, 62, 505–528.

Jeanloz, R. and Lay, T. (1993) The Core-Mantle Boundary. Scientific American, 268, 26–33.

Knittle, E. and Jeanloz, R. (1986) High-pressure metallization of FeO and implications for the earth's core. Geophysical Research Letters, 13, 1541–1544.

Mackrodt, W.C., Harrison, N.M., Saunders, V.R., Allan, N.L., Towler, M.D., Apra, E., and Dovesi, R. (1993) Ab initio Hartree-Fock calculations of CaO, VO, MnO and NiO. Philosophical Magazine A (Physics of Condensed Matter), 68, 653–666.

Manga, M. and Jeanloz, R. (1996) Implications of a metal-bearing chemical boundary layer in D″ for mantle dynamics. Geophysical Research Letters, 23, 3091–3094.

Mazin, I.I. and Anisimov, V.I. (1997) Insulating gap in FeO: Correlations and covalency. Physical Review, B55, 12822–12825.

Mazin, I.I. and Singh, D. (1997) Electronic structure and magnetism in Ru-based perovskites. Physical Review, B56, 2556–2573.

Pasternak, M.P., Taylor, R.D., Jeanloz, R., Li, X., Nguyen, J.H., and McCammon, C.A. (1997) High pressure collapse of magnetism in $Fe_{0.94}O$: Mössbauer spectroscopy beyond 100 GPa. Physical Review Letters, 79, 5046–5049.

Perdew, J.P. and Wang, Y. (1992) Accurate and simple analytic representation of the electron-gas correlation energy. Physical Review, B45, 13244–13249.

Rai, R.S., Singh, S.R., Dubey, M., and Singh, G. (1986) Lattice imaging studies on structure and disorder in SiC polytypes. Bulletin de Mineralogie, 109, 509–527.

Reynolds, R.C. (1985) NEWMOD, a computer program for the calculation of one-dimensional diffraction patterns of mixed-layered clays. R.C. Reynolds, Hanover, New Hampshire.

Sherman, D.M. and Jansen, H. (1995) First-principles prediction of the high-pressure phase transition and electronic structure of FeO; implications for the chemistry of the lower mantle and core. Geophysical Research Letters, 22, 1001–1004.

Singh, D.J. (1994) Planewaves, Pseudopotentials, and the LAPW Method, 115 p. Kluwer Academic Publishers, Boston.

Szotek, Z. and Temmerman, W.M. (1993) Application of the self-interaction correction to transition-metal oxides. Physical Review, B7, 4029–4032.

Takahashi, M. and Igarashi, J. (1996) Local approach to electronic excitations in MnO, FeO, CoO, and NiO. Physical Review, B54, 13566–13574.

Wei, S.H. and Krakauer, H. (1985) Local density functional calculation of the pressure induced phase transition and metallization of BaSe and BaTe. Physical Review Letters, 55, 1200–1203.

Yagi, T., Suzuki, K., and Akimoto, S. (1985) Static compression of wüstite ($Fe_{0.98}O$) to 120 GPa. Journal of Geophysical Research, 90, 8784–8788.

Manuscript received November 6, 1997
Manuscript accepted December 26, 1997
Paper handled by Anne M. Hofmeister